

## Supporting Information

### **Thermally activated delayed fluorescence emitters with low concentration sensitivity for highly efficient organic light emitting devices**

Xiao-Chun Fan,<sup>a</sup> Kai Wang,<sup>\*a</sup> Cai-Jun Zheng,<sup>\*b</sup> Gao-Le Dai,<sup>a</sup> Yi-Zhong Shi,<sup>a</sup> Yan-Qing Li,<sup>a</sup> Jia Yu,<sup>a</sup> Xue-Mei Ou<sup>a</sup> and Xiao-Hong Zhang<sup>\*a</sup>

a. Institute of Functional Nano & Soft Materials (FUNSOM), Jiangsu Key Laboratory for Carbon-Based Functional Materials & Devices, Soochow University, Suzhou Jiangsu, 215123, P.R. China.

\*Email: xiaohong\_zhang@suda.edu.cn; wkai@suda.edu.cn

b. School of Optoelectronic Science and Engineering, University of Electronic Science and Technology of China, Chengdu, Sichuan, 610054, P.R. China. \*Email: zhengcaijun@uestc.edu.cn

## 1. Materials and Measurements

All reagents were purchased from commercial sources and used without further purification. 9-([1,1'-biphenyl]-2-yl)-2,7-dibromo-9H-thioxanthen-9-ol **3**, 2',7'-dibromospiro[fluorene-9,9'-thioxanthene] **4**, 2',7'-dibromospiro[fluorene-9,9'-thioxanthene] 10',10'-dioxide **5** were prepared with the similar synthetic method in following literature procedures.

$^1\text{H}$  NMR and  $^{13}\text{C}$  NMR spectra were recorded on a Bruker 600 MHz spectrometer in suitable deuterium reagent in room temperature, and different solvents, such as  $d_6$ -acetone,  $d_6$ -DMSO and  $\text{CDCl}_3$  were used based on the solubility of the measured compounds. Thermogravimetric analysis (TGA) curve was carried on a Perkin Elmer at a heating rate of  $10\text{ }^\circ\text{C}\cdot\text{min}^{-1}$  from 50 to  $550\text{ }^\circ\text{C}$  under nitrogen. Differential scanning calorimetry (DSC) curve was carried on a TA DSC 2010 unit at a heating rate of  $10\text{ }^\circ\text{C}\cdot\text{min}^{-1}$  from 25 to  $350\text{ }^\circ\text{C}$  under nitrogen. The temperature of 5% weight loss was defined as the decomposition temperature ( $T_d$ ). Cyclic voltammetry (CV) curve was recorded on a CHI660C electrochemistry station in DMF solution with tetrabutylammonium hexafluorophosphate ( $\text{Bu}_4\text{NPF}_6$ ) at a scan rate of  $100\text{ mV}\cdot\text{s}^{-1}$ . Ultraviolet absorption spectrum was obtained on a Jasco V-570 UV-vis spectrometer Edinburgh Instruments F980.

*Theoretical Calculation:* The orbital distributions of the highest occupied molecular orbital (HOMO) and the lowest occupied molecular orbital (LUMO) of the optimized ground state and excited state were calculated with the time-dependent density function theory (TD-DFT) using B3LYP/6-31g(d) basis set in Gaussian 09 program package. The natural transition orbitals (NTOs) analysis were further visualized with a multifunctional wavefunction analyzer (Multiwfn).<sup>1</sup>

## 2. Synthesis and characterization

The compound 2,7-dibromo-9H-thioxanthen-9-one **1** and 2-bromo-1,1'-biphenyl **2** were purchased from commercial sources and used without further purification. The synthesis of compound **3**, compound **4** and compound **5** were refer to the reported

literature.<sup>2</sup>

**Synthesis of 9-([1,1'-biphenyl]-2-yl)-2,7-dibromo-9H-thioxanthen-9-ol (3).** 2-bromo-1,1'-biphenyl (699 mg, 3mmol) was added into 30mL ultra dry tetrahydrofuran and cooled to -78°C under nitrogen. Then n-Butyllithium (1.9 mL, 1.6 mol/L) was slowly added dropwise and stirred for 2h. 2,7-dibromo-9H-thioxanthen-9-one (741 mg, 2 mmol) dissolved in extra 50ml ultra dry tetrahydrofuran was added in same temperature. After stirring for extra 2 h, the mixture was moved to room temperature and stirring for 10h. The mixture was added in 500 mL H<sub>2</sub>O and filtered to get a white solid. The crude product was further purified by silica gel column and dried under vacuum to afford compound **3** (870 mg, 87%). <sup>1</sup>H NMR (600 MHz, *d*<sub>6</sub>-acetone, ppm): δ 7.55-7.49 (m, 3H), 7.43 (dd, *J* = 5.8, 3.4 Hz, 2H), 7.40 (dd, *J* = 8.4, 2.2 Hz, 2H), 7.25 (t, *J* = 7.5 Hz, 1H), 7.22 (d, *J* = 8.4 Hz, 2H), 7.10 (t, *J* = 7.7 Hz, 2H), 7.03 (dd, *J* = 5.7, 3.3 Hz, 1H), 6.53 (d, *J* = 7.3 Hz, 2H), 4.85 (s, 1H). Found: *m/z* 524.20.

**Synthesis of 2',7'-dibromospiro[fluorene-9,9'-thioxanthene] (4).** Compound **3** (787 mg, 1.5 mmol) was added into mixed acid solution (5 ml acetic acid and 0.2 ml hydrochloric acid) and stirred at 80°C for 24h. The cooled mixture was filtered directly to get pale solid and further precipitated by Hexane/DCM and dried under vacuum to afford compound **4** (647 mg, 85%). <sup>1</sup>H NMR (600 MHz, *d*<sub>6</sub>-acetone, ppm): δ 8.04 (d, *J* = 7.7 Hz, 2H), 7.61 (t, *J* = 8.0 Hz, 4H), 7.53-7.47 (m, 4H), 7.43 (t, *J* = 7.6 Hz, 2H), 6.63 (d, *J* = 2.0 Hz, 2H). Found: *m/z* 506.20.

**Synthesis of 2',7'-dibromospiro[fluorene-9,9'-thioxanthene] 10',10'-dioxide (5).** A mixture of compound **4** (506 mg, 1 mmol), 10 ml acid solution and 1.5ml H<sub>2</sub>O<sub>2</sub> was stirred at 108°C for 24h. The cooled system was added to 50ml H<sub>2</sub>O and filtered to get a white solid. The crude product was further purified by silica gel column and dried under vacuum to afford compound **5** (527 mg, 98%). <sup>1</sup>H NMR (600 MHz, *d*<sub>6</sub>-DMSO, ppm): δ 8.14 (d, *J* = 8.5 Hz, 2H), 8.09 (d, *J* = 7.7 Hz, 2H), 7.82 (dd, *J* = 8.6, 1.9 Hz, 2H), 7.52 (t, *J* = 7.3 Hz, 2H), 7.35-7.30 (m, 4H), 6.49 (d, *J* = 1.9 Hz, 2H). Found: *m/z*

538.20.

**Synthesis of 2',7'-di(10H-phenoxazin-10-yl)spiro[fluorene-9,9'-thioxanthene] 10',10'-dioxide (SPFS-PXZ).** Compound 5 (430 mg, 0.8 mmol), 10H-phenoxazine (329 mg, 1.8 mmol), Sodium tert-butoxide (307 mg, 3.2 mmol), Palladium acetate (18 mg, 0.08 mmol), Tri-tert-butyl phosphine (0.4 ml, 0.16 mmol) were added into 30 ml toluene and stirred at 110°C under nitrogen for 24h. The cooled mixture was filtered directly and the residue was wash with plenty of water to get dark green solid. The crude product was recrystallized form DCM and further purified by vacuum distillation to afford green solid (450 mg, 76%). <sup>1</sup>H NMR (600 MHz, CDCl<sub>3</sub>, ppm): δ 8.44 (d, J = 8.5 Hz, 2H), 7.74 (d, J = 7.6 Hz, 2H), 7.51-7.49 (m, 2H), 7.39 (dd, J = 12.9, 7.6 Hz, 4H), 7.23 (s, 2H), 6.60 (d, J = 4.4 Hz, 8H), 6.56 (d, J = 1.8 Hz, 2H), 6.45 (dt, J = 8.6, 4.6 Hz, 4H), 5.67 (d, J = 8.1 Hz, 4H). HRMS (EI). Calcd for C<sub>49</sub>H<sub>30</sub>N<sub>2</sub>O<sub>4</sub>S (M<sup>+</sup>): 743.8490. found: 743.8478. <sup>13</sup>C NMR cannot be obtained due to poor solubility.

### 3. Thermodynamic analysis

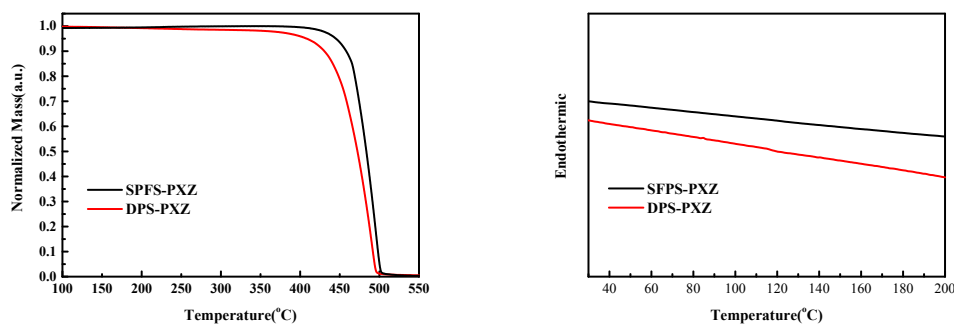


**Figure S1.** TGA (left) and DSC (right) curve of **SPFS-PXZ** and **DPS-PXZ**

## 4. Computational data

**Table S1.** Calculated  $E_{VA}(S_1)$  and  $E_{VA}(T_1)$  using various exchange-correlation functionals and 6-31G\* basis set based on B3LYP optimized geometries, and calculated CT amount ( $q$ ), optimal HF% (OHF),  $E_{0-0}(^1CT)$  and  $E_{0-0}(^3CT)$  of the compounds.

parameter	functional	DPS-PXZ <sup>f</sup>	SPFS-PXZ
$E_{VA}(S_1)$ (eV)	B3LYP <sup>3,4</sup>	2.4452	2.6003
	PBE0 <sup>5,6</sup>	2.6154	2.7651
	MPW1B95 <sup>7</sup>	2.7834	2.9184
	BMK <sup>8</sup>	3.1189	3.2408
	M06-2X <sup>9</sup>	3.3545	3.4566
	M06-HF <sup>10</sup>	4.0808	4.1597
$E_{VA}(T_1)$ (eV)	B3LYP	2.4147	2.5795
	PBE0	2.5744	2.7337
	MPW1B95	2.7465	2.8923
	BMK	3.0699	3.0857
	M06-2X	3.2706	3.2700
	M06-HF	3.6352	3.6380
CT amount (e) <sup>a</sup>		0.861	0.881
optimal HF% <sup>b</sup>		36	37
$E_{VA}(S_1, OHF)$ (eV) <sup>c</sup>		2.95	3.15
$E_{0-0}(^1CT)$ (eV) <sup>d</sup>		2.71	2.91
$E_{0-0}(^3CT)$ (eV) <sup>e</sup>		2.66	2.89

<sup>a</sup> Orbital compositions were analyzed using Multiwfn.<sup>1</sup> <sup>b</sup>  $OHF = 42q$ .<sup>11</sup> <sup>c</sup> The  $E_{VA}(S_1)$  corresponding to the OHF can be read from the best fit straight line for a double log plot of  $E_{VA}(S_1)$  against HF% (see Figure S9). <sup>d</sup>  $E_{0-0}(^1CT) = E_{VA}(S_1, OHF) - 0.24$  eV.<sup>10</sup> <sup>e</sup>  $E_{0-0}(^3CT) = E_{0-0}(S_1) - E_{VA}(S_1, OHF) + E_{VA}(S_1, OHF)/E_{VA}(S_1, B3LYP) \times E_{VA}(T_1, B3LYP)$ .<sup>10</sup> <sup>f</sup> Calculated data were refer to the reported literature.<sup>12</sup>

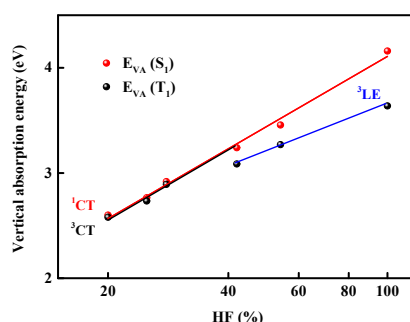


**Figure S2.** Dependence of  $E_{VA}(S_1)$  and  $E_{VA}(T_1)$  on the HF% in TD-DFT for SPFS-PXZ, plotted on a log-log scale.

## 5. Electrochemical measurements

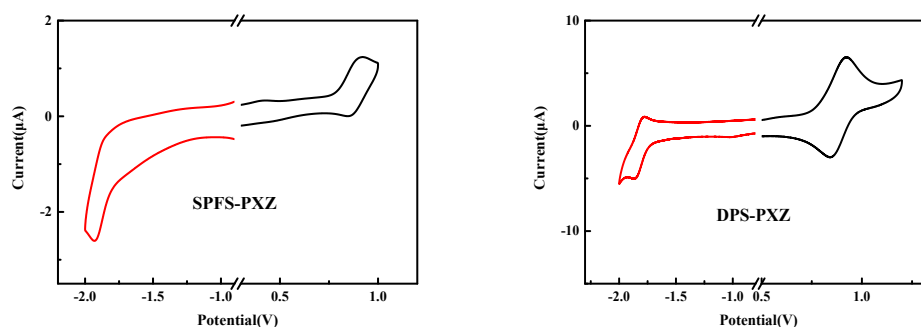


**Figure S3.** Cyclic voltammetry curves of **SPFS-PXZ** (left) and **DPS-PXZ** (right) in DMF.

## 6. Photophysical properties

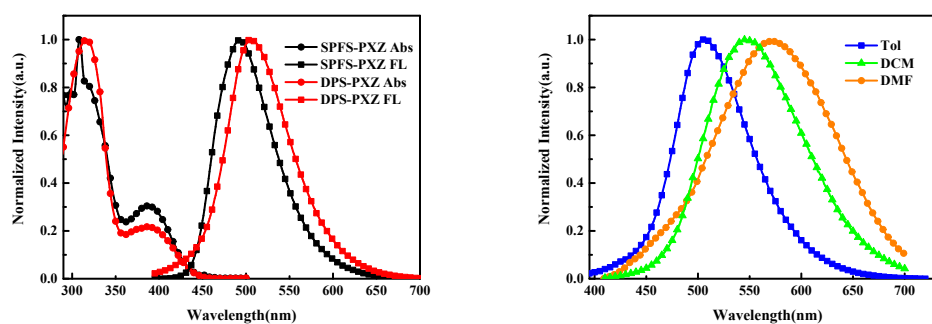


**Figure S4.** The UV-Vis absorption and fluorescence spectra (left) of **SPFS-PXZ** (black) and **DPS-PXZ** (red) in toluene at room temperature; and fluorescence spectra (right) of **DPS-PXZ** in different polar solvents: toluene (blue), dichloromethane (green), dimethyl formamide (orange).

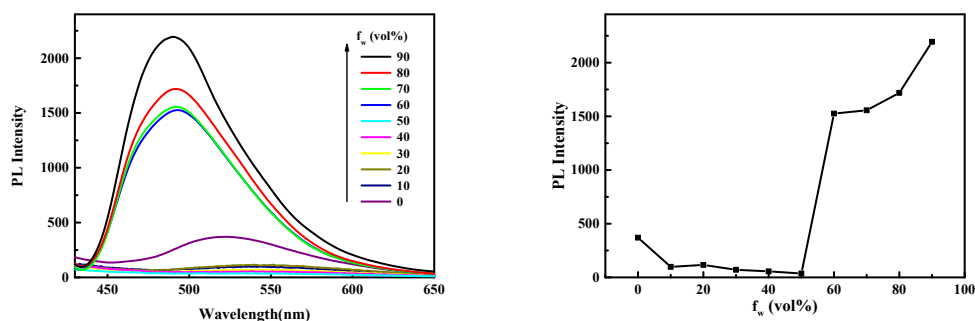


**Figure S5.** Fluorescence spectra (left) of **SPFS-PXZ** in THF/water mixtures with different water fractions ( $f_w$ ) and fluorescence intensity -  $f_w$  curve (right).

**Table S2.** Photophysical parameters of SPFS-PXZ and DPS-PXZ in different solvent.

Compound	Solvent	Tol	DCM	DMF
DPS-PXZ	$\lambda_{em}^a$ [nm]	507	546	572
	Stokes shift [nm]	117	156	182
	FWHM <sup>b</sup> [nm]	84	112	137
SPFS-PXZ	$\lambda_{em}^a$ [nm]	492	524	564
	Stokes shift [nm]	102	134	174
	FWHM <sup>b</sup> [nm]	80	96	122

<sup>a</sup> maximum wavelength of fluorescence spectrum. <sup>b</sup> Full Width at Half-Maximum.

## 7. Electroluminescence performance.

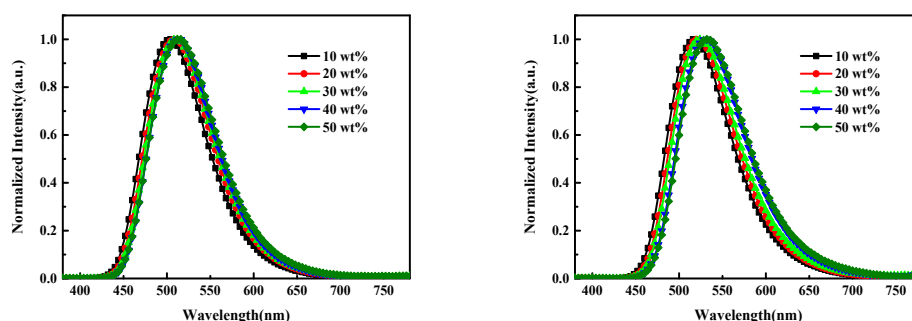


**Figure S6.** EL spectra of SPFS-PXZ (left) and DPS-PXZ (right) -doped devices for different doping concentration at  $1000 \text{ cd}\cdot\text{m}^{-2}$ .

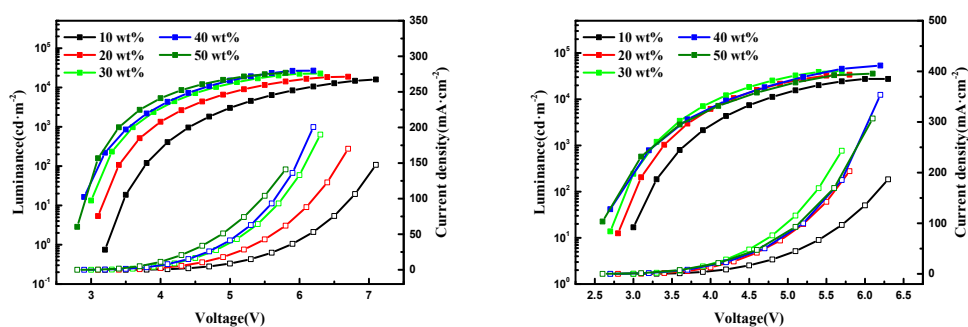


**Figure S7.** Voltage-Luminance-Current density characteristics of SPFS-PXZ (left) and DPS-PXZ (right) -doped devices for different doping concentration.

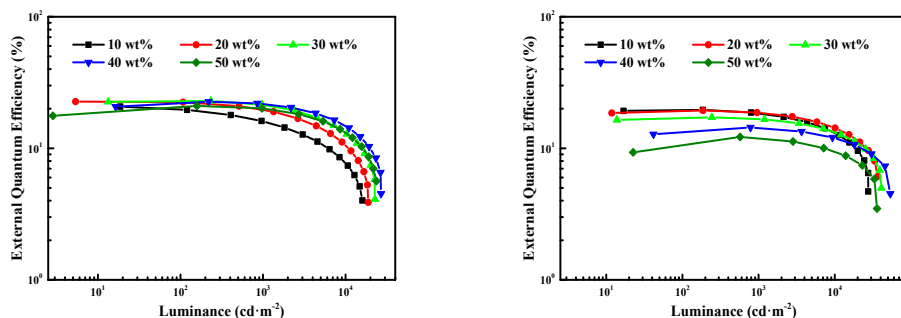


**Figure S8.** EQE of SPFS-PXZ (left) and DPS-XPZ (right) -doped devices for different doping concentration.

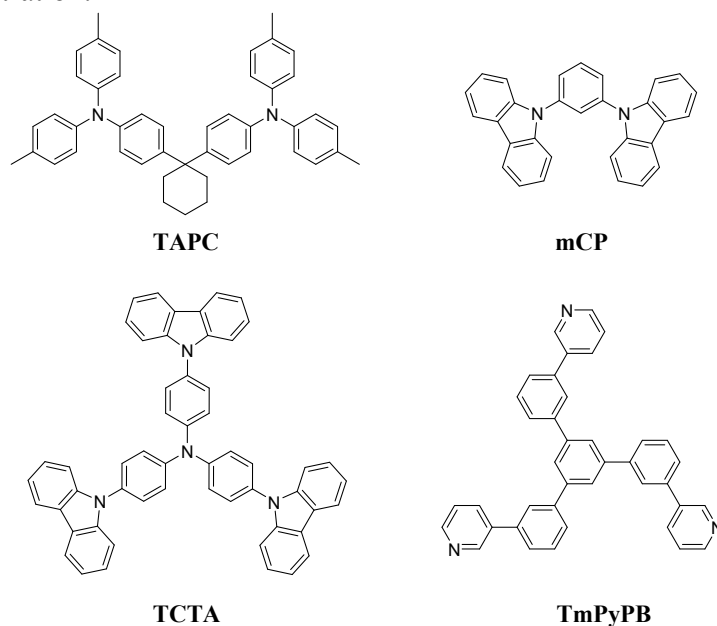


**Figure S9.** The molecular structure of materials applied in devices.

## 8. Reference

1. T. Lu and F. Chen, *J. Comput. Chem.*, 2012, **33**, 580-592.
2. Y. Li, Z. Wang, X. Li, G. Xie, D. Chen, Y.-F. Wang, C.-C. Lo, A. Lien, J. Peng, Y. Cao and S.-J. Su, *Chem. Mater.*, 2015, **27**, 1100-1109.
3. A. D. Becke, *J. Chem. Phys.*, 1993, **98**, 5648-5652.
4. P. J. Stephens, F. J. Devlin, C. F. Chabalowski and M. J. Frisch, *The Journal of Physical Chemistry*, 1994, **98**, 11623-11627.
5. J. P. Perdew, Burke, K. & Ernzerhof, M., *Phys. Rev. Lett.*, 1995, **77**, 3865-3868.
6. C. S. Adamo, G. E., *J. Chem. Phys.*, 1999, **111**, 2889-2899.
7. Y. Zhao and D. G. Truhlar, *The Journal of Physical Chemistry A*, 2004, **108**, 6908-6918.
8. A. D. M. Boese, J. M. L., *J. Chem. Phys.*, 2004, **121**, 3405-3416.
9. Y. Zhao and D. G. Truhlar, *Theor. Chem. Acc.*, 2007, **120**, 215-241.
10. Y. Zhao and D. G. Truhlar, *J. Phys. Chem. A*, 2006, **110**, 13126-13130.
11. S. Huang, Q. Zhang, Y. Shiota, T. Nakagawa, K. Kuwabara, K. Yoshizawa and



- C. Adachi, *J. Chem. Theory Comput.*, 2013, **9**, 3872-3877.
12. Q. Zhang, B. Li, S. Huang, H. Nomura, H. Tanaka and C. Adachi, *Nature Photonics*, 2014, **8**, 326-332.